complexes prepared from mixtures of I(1,14) and oleic acid also exhibited an increase in W as the ratio of the bound ligand (SLFA plus oleic) to protein was increased. The contribution of bound–free ligand exchange to W cannot be assessed from the EPR data but is probably negligible. Dissociation rate constants for oleate–human serum albumin (HSA) complexes have been measured to be approximately 3×10^{-2} s^{-1} (Scheider, 1980). A line-width contribution of this magnitude is insignificant compared to the intrinsic line width which conservatively is 10^{-7} s^{-1} (i.e., $1/T_2 = 10^7$ s^{-1} + 10^{-2} s^{-1} $\approx 10^7$ s^{-1}).

Although a precise physical interpretation cannot be made, the changes in W indicate an inhomogeneity of the low-affinity binding sites which is not reflected in detectable changes in the association constants.

Mobility of Bound SLFA. Figure 6 summarizes in graphic form the estimates of mobility of the nitroxyl radical attached to different positions along the carbon chain of stearate when bound to the highest affinity site(s) on BSA. The estimates by three different experimental approaches are in agreement and suggest that the central portion of the bound SLFA is more rigidly attached to BSA than is either terminus. This differs from the suggestion of Morrisett et al. (1975) that the SLFA is bound to the protein near the carboxyl end of the fatty acid chain. Either suggestion, however, would be valid only if the three SLFA bound to the same site(s) on the BSA. As discussed above, this is not established because of the uncertainties in interpreting differences in binding affinities. Furthermore, suggestions with regard to segmental binding of SLFA to binding of the natural FA are subject to the additional problem that the steric hindrance of the nitroxyl radical is maximal in the segment of FA for which information regarding mobility is sought.

References

Abumrad, N. A., Perkins, R. C., Park, J. H., & Park, C. R. (1981) *J. Biol. Chem. 256*, 9183–9191.

Beth, A. H., Wilder, R. T., Wilkerson, L. S., Perkins, R. C., Meriwether, B. P., Dalton, L. R., Park, C. R., & Park, J. H. (1979) *J. Chem. Phys. 71*, 2074–2082.

Freed, J. H. (1976) in *Spin Labeling, Theory and Applications* (Berliner, L. J., Ed.) Vol. 1, pp 53–130, Academic Press, New York.

Mc Calley, R. C., Schimshick, E. J., & Mc Connell, H. M. (1972) *Chem. Phys. Lett. 13*, 115–117.

Morrisett, J. D., Pownall, H. J., & Gotto, A. M. J. (1975) *J. Biol. Chem. 250*, 2487–2494.

Rehfield, S. J., Eatough, D. J., & Plachy, W. Z. (1978) *J. Lipid Res. 19*, 841–849.

Scatchard, G. (1949) *Ann. N.Y. Acad. Sci. 51*, 660–672.

Scheider, W. (1980) *J. Phys. Chem. 84*, 925–928.

Spector, A. A. (1975) *J. Lipid Res. 16*, 165–179.

Spector, A. A., & Hock, J. L. (1969) *Anal. Biochem. 32*, 297–302.

Spector, A. A., & Fletcher, J. (1978) in *Disturbances in Lipid and Lipoprotein Metabolism* (Dietschy, J. M., Gotto, A. M., & Ontko, J. A., Eds.) pp 229–240, Waverly Press, Inc., Baltimore, MD.

Spector, A. A., John, K., & Fletcher, J. E. (1969) *J. Lipid Res. 10*, 56–67.

Thomas, D. D., Dalton, L. R., & Hyde, J. S. (1976) *J. Chem. Phys. 65*, 3006–3024.

Flexibility of Myosin Rod Determined from Dilute Solution Viscoelastic Measurements†

Søren Hvidt, F. Henry M. Nestler, Marion L. Greaser, and John D. Ferry*

ABSTRACT: The frequency dependences of the storage and loss shear moduli, G' and G'', of myosin rod solutions at 1.0 and 7.0 °C were measured by use of the Birnboim-Schrag multiple lumped resonator apparatus in solvents with and without glycerol. The infinite dilution moduli were determined and compared with theoretical models for a rigid rod and a freely jointed trinodular rod and with an empirical model for a semiflexible rod. Only the latter could fit the data. A rotational relaxation time of 25 μs and a slowest bending time of 3.1 μs, both reduced to water at 20 °C, were determined from the fit. A persistence length of about 130 nm was obtained from either the bending time, the rotational relaxation time, or the intrinsic viscosity. The average thermal excursion of the end of subfragment 2 was estimated to be 26 nm, more than sufficient to span the gap between the thick and thin filaments in muscles at all sarcomere lengths. Thus, a hinge between heavy meromyosin and light meromyosin does not appear necessary for myosin–actin contact. Young's modulus of about 1×10^9 N/m^2 also makes it unlikely that subfragment 2 can be the elastic element in the Huxley–Simmons model of muscle contraction.

Current theories of muscle contraction suppose that force generation occurs through an interaction between myosin in the thick filaments and actin in the thin filaments (Harrington, 1979a). The detailed mechanism of force generation is not well understood but is hypothesized to involve either a rotation of the myosin heads when they are attached to the thin filaments (Huxley & Simmons, 1971) or a helix–coil transition in the helical part of myosin (Harrington, 1979b). Both models involve a step in which the myosin heads swing out from their resting position in the vicinity of the surface of the thick filaments and become attached to the thin filaments. The distance between the myosin head at rest and the surface of the thin filament is believed to be about 5–6 nm (Harrington, 1979a). Thus, a substantial radial movement would be re-

† From the Department of Chemistry and the Muscle Biology Laboratory, University of Wisconsin—Madison, Madison, Wisconsin 53706. *Received March 5, 1982.* This research was supported by Grants GM-21652 (to J.D.F.) and HL-18612 (to M.L.G.) from the National Institutes of Health and by the College of Agricultural and Life Sciences. S.H. appreciates travel support from the Danish Science Foundation.

0006-2960/82/0421-4064$01.25/0

quired to allow attachment of myosin heads to actin. Such a movement would necessitate flexibility of myosin in its helical part. A recent determination of the fraction of myosin heads bound to actin in rigor seems to require even more mobility of the myosin heads than just the radial distance between the filaments (Lovell & Harrington, 1981).

Much information about the physical and biochemical properties of myosin has been obtained from studies of myosin fragments. Myosin consists of a long double-stranded coiled-coil α-helical part, myosin rod, connected at one end to two globular heads (Lowey, 1971). Various proteolytic enzymes cleave myosin into fragments. Trypsin and chymotrypsin cleave near the middle of the helical part to give light meromyosin (LMM)[1] and heavy meromyosin (HMM), whereas papain shows a higher tendency to cleave between the rod and the globular heads (S-1) (Weeds & Pope, 1977). Further digestion of the rod with trypsin results in LMM and the rest of the helical fraction called subfragment 2 (S-2). Subfragment 1 contains the actin binding and ATPase active sites. The role of LMM seems to be explained by its tendency to aggregate, thereby anchoring myosin into the thick filament (Harrington & Burke, 1972). The function of S-2 is less clear. The main portion of S-2 shows little tendency to aggregate even at low ionic strength (Sutoh et al., 1978). This evidence suggests that HMM could disengage and swing away for thick filament during the contraction cycle.

The proteolytic vulnerability at the S-1/S-2 and S-2/LMM junctions has been taken as an indication of flexibility in these regions. There seems to be convincing experimental evidence for a "swivel" at the S-1/S-2 junction based on fluorescence depolarization measurements (Mendelson et al., 1973) and other spectroscopic techniques (Thomas et al., 1975; Kobayashi & Totsuka, 1975). A hinge near the S-2/LMM junction was postulated by Huxley (1969). The temperature dependence of the helical content and of the specific viscosity of the rod has been interpreted in support of such a hinge (Burke et al., 1973). The results of calorimetric measurements have also been taken as evidence for a hinge at physiological temperatures (Swenson & Ritchie, 1980). Electrooptical measurements of rod, LMM, and S-2 were interpreted to show flexibility in the part of S-2 adjacent to LMM even at 3 °C (Highsmith et al., 1977). Fluorescence depolarization studies, however, showed little or no flexibility in the rod up to 40 °C at neutral pH (Harvey & Cheung, 1977).

Measurements of the dilute solution viscoelastic properties for a wide variety of macromolecules have been performed in recent years in this laboratory (Ferry, 1978, 1980). Information about the shape and the dynamics of macromolecules can be obtained from the frequency dependence of the complex shear modulus (or, equivalently, the complex viscosity). The results for semiflexible rods have provided information about rotational relaxation times together with relaxation times for internal motions. Myosin has been studied (Rosser et al., 1978), but the interpretation was complicated by the presence of the head portions of the molecule. Low-temperature viscoelastic measurements of myosin rod are reported here. The viscoelastic data will be compared with various theoretical models, and the significance of the results in terms of muscle contraction will be discussed.

[1] Abbreviations: LMM, light meromyosin; HMM, heavy meromyosin; S-1, myosin subfragment 1; S-2, myosin subfragment 2; NaDodSO$_4$, sodium dodecyl sulfate; Tris, 2-amino-2-(hydroxymethyl)-1,3-propanediol; ATP, adenosine 5′-triphosphate; EDTA, ethylenediaminetetraacetic acid; CD, circular dichroism; DEAE, diethylaminoethyl; g, acceleration of gravity; DNA, deoxyribonucleic acid; UV, ultraviolet; HAP, hydroxylapatite.

The question of the flexibility of myosin rod has recently been carefully reviewed by Harvey & Cheung (1982). They summarize that different investigators have reached very different conclusions. They favor a model in which the rod can bend slightly against an elastic force. We find that the rod is a semiflexible rod with a persistence length of 130 nm. This value is very high and shows that the rod is quite stiff, but due to the long length of the rod, considerable bending motions are allowed.

Experimental Procedures

Materials. All chemicals were of reagent grade or better. Glycerol (99+%) was purchased from Aldrich Chemical Co. Twice-recrystallized papain and 2-iodoacetamide were obtained from Sigma Chemical Co. A set of high molecular weight standards for gel electrophoresis was obtained from Bio-Rad. Twice-distilled water was used throughout.

Preparation of Myosin Rod. Myosin rod was prepared from rabbit skeletal muscle by adaptation of the methods of Oriol et al. (1973), Lowey et al. (1969), and Harrington & Burke (1972). All steps were carried out at 4 °C unless otherwise stated.

Leg and back muscle (primarily white muscle) was ground and suspended in 4 volumes of 0.1 M KCl, 50 mM imidazole (pH 6.6), and 20 mM EDTA. The mixture was then filtered with cheesecloth, and the residue was resuspended in 4 volumes of 0.1 M KCl, 50 mM imidazole (pH 6.6), and 10 mM EDTA. The suspension was filtered, and the washing was repeated once more. The muscle residue was resuspended in 3 volumes of the same buffer, blended 30 s in a large Waring Blendor, and centrifuged at 2000g for 20 min. The supernatant was discarded. This step was repeated twice with a filtration through cheesecloth before the last centrifugation to remove connective tissue and undisrupted muscle chunks. The myofibrils were then resuspended in 5 volumes (relative to original muscle weight) of 0.05 M KCl, 25 mM imidazole (pH 6.6), 5 mM EDTA, and 1 mM dithiothreitol. Papain was activated as described by Lowey et al. (1969). The suspension was then digested with gentle stirring for 20 min at 23 °C with a 1:7000 papain:original muscle weight ratio (approximately 1:700 papain:myofibril protein). The digestion was quenched by adding iodoacetamide, $MgCl_2$, and sodium pyrophosphate to a final concentration of 2 mM each. The suspension was centrifuged at 16000g for 40 min, and the pellet was resuspended in 1 M KCl and 10 mM EDTA (pH 7.3) to make a final concentration of 0.6 M KCl. Three volumes of ethanol were added slowly over 20 min with continuous stirring (Harrington & Burke, 1972). The suspension was centrifuged at 2000 g for 10 min, and the pellet was dialyzed against large volumes of 0.5 M KCl, 10 mM EDTA, and 0.2 M potassium phosphate (pH 7.3) overnight. The suspension was centrifuged at 35000g for 20 min, and the pellet was discarded. The supernatant (containing myosin rod and some tropomyosin) was dialyzed against 20 mM KCl and 10 mM phosphate (pH 6.0). Tropomyosin is soluble under these conditions whereas rod precipitates. The pellet, after a centrifugation at 35000g for 20 min, was dissolved in 0.5 M KCl, 0.5 M phosphate (pH 7.3), and 10 mM EDTA. This solvent was used for most physical measurements and will be referred to as buffer A. The solution was clarified at 100000g for 2 h, resulting in a crude stock solution.

Rod solutions were often concentrated by dropwise addition of 2 N HCl with continuous stirring until the pH was lowered to 4.8, followed by a centrifugation at 10000g for 20 min. The rod-containing pellet was then transferred to a dialysis bag with a minimum amount of buffer A, dialyzed until dissolved,

and clarified by high-speed centrifugation, as above.

Column Purification. The crude stock solutions often showed lower molecular weight contaminants when analyzed on $NaDodSO_4$–polyacrylamide gels. Two new column purification techniques were used to reduce the amounts of these contaminants before any physical measurements were made. In the first, about 300 mg of rod was dialyzed vs. 0.5 M KCl, 25 mM phosphate (pH 7.0), and 15 mM β-mercaptoethanol and applied to a column (9-cm length, 5-cm diameter) of hydroxylapatite (Bio-Rad) equilibrated with the same solvent. Elution was performed with a linear gradient made from 800 mL of initial solvent and 800 mL of 0.5 M KCl, 0.5 M phosphate (pH 7.0), and 15 mM β-mercaptoethanol. The flow rate was 70 mL/h, and the cleanest fractions of the somewhat asymmetric peak were pooled. Myosin rod purified in this way will be referred to as "native rod" in the following.

For the other method, a DEAE-cellulose (Whatman DE-52) column (length 17 cm, diameter 4 cm) with 7 M urea was used to obtain rod preparations with little or no contaminants. About 500 mg of rod was dialyzed vs. 7 M urea (freshly deionized)–25 mM Tris (pH 8.0)–15 mM β-mercaptoethanol and applied to the column preequilibrated in the same solvent. A linear gradient with 800 mL of initial solvent and 800 mL of initial solvent plus 0.1 M KCl was used. The flow rate was 70 mL/h. The back two-thirds of the main peak was pooled and dialyzed 6 times vs. 10 volumes of buffer A over 36 h. The first three dialysis solvents contained also 1 mM dithiothretiol. The renaturation of the rod appeared to take place during the first dialysis, as judged from a significant increase in solution viscosity. Rod preparations purified according to this scheme will be referred to as "renatured rod".

Sample Storage. Rod solutions were stored in buffer A at 0 °C for up to 10 days during a series of experiments. Solutions were stored for up to 2 months in a mixture of 1 volume of buffer A and 2 volumes of ethanol at −20 °C. Stored samples were dialyzed vs. large volumes of buffer A and clarified by centrifugation at 100000*g*.

Gel Electrophoresis. Polyacrylamide tube stacking gels (6-mm inner diameter and 13 cm by length) with sodium dodecyl sulfate were used essentially as described by Laemmli (1970). A Tris–glycine buffer system was used, and the ratio of acrylamide to methylenebis(acrylamide) was 37.5 to 1. The separating and stacking gels contained 8 and 4.5% acrylamide, respectively. Samples were incubated at 100 °C for 3 min in 3% $NaDodSO_4$, 30% glycerol, and 2% dithiothreitol. Electrophoresis was done at 20 °C with 1 mA/gel for 1 h followed by 2.5 mA/gel for about 4 h. Gels were stained with Coomassie Brilliant Blue and destained in 7% methanol and 14% acetic acid. Gels were scanned at 570 nm on a Gilford spectrophotometer equipped with a gel scanning device. The relative amounts of protein were estimated from the areas under the absorption peaks. The areas were estimated from peak height times half-width. Apparent molecular weights were estimated by comigrating rod samples with high molecular weight standards obtained from Bio-Rad.

Solvents. Two solvents were used for the viscoelastic measurements: the aqueous solvent (buffer A) and a solvent that contained the same concentration of salts together with 0.6 M glycine and 50.6% glycerol by weight (buffer G). Solvents and rod solutions containing glycerol were made up in two steps. Buffer G solvent was obtained by mixing buffer A with a 68% glycerol solution which contained the rest of the salts and glycine. The rod solutions in buffer G were made by adding the same relative amount of 68% glycerol to a rod solution in buffer A. The solutions were then dialyzed against buffer G with at least two changes of solvent for 48 h. A similar solvent was used for the previous viscoelastic measurements of myosin (Rosser et al., 1978).

Viscosity and Density Determinations. The viscosities of buffer A and buffer G were measured with Cannon-Fenske 50 and 150 viscometers, respectively, in a thermostated bath (±0.1 °C). Densities were determined by the use of a 25-mL pycnometer. Instrinsic viscosities of the rod in buffer A were measured in a Cannon-Fenske 50 viscometer after some preliminary measurements showed no shear-rate dependence. A Cannon-Ubbelohde four bulb shear dilution type viscometer was used for the rod solutions in buffer G at 7.0 °C. About a 4% decrease in specific viscosity was observed in the shear-rate range from 8 to 42 s^{-1}, and the zero shear-rate specific viscosity was found from a short extrapolation. The intrinsic zero shear-rate viscosity was then obtained from a linear extrapolation to zero concentration. The intrinsic viscosity at 1.0 °C was assumed to be the same as the value measured at 7.0 °C.

Concentration Measurements. A differential refractive index at 546 nm of 0.177 mL/g corresponding to 39 fringes/1% (Harrington & Burke, 1972) was used as a calibration to obtain an extinction coefficient at 278 nm. A Brice differential refractometer was calibrated with KCl and sucrose solutions. A series of rod solutions in buffer A were then measured in both the refractometer and a Gilford spectrophotometer. The measured absorption at 278 nm was corrected for the measured scattered light at 320 nm (Houk & Ue, 1974). The extinction coefficient at 278 nm was found to be 0.21 L/(g·cm) based on concentrations from the differential refractometer. This value is in good agreement with the value of 0.20 L/(g·cm) found by Harrington & Himmelfarb (1972) and a more recent value of 0.22 L/(g·cm) at 280 nm (Margossian et al., 1981). An extinction coefficient of 0.21 L/(g·cm) at 278 nm was used in all subsequent concentration determinations.

Viscoelastic Measurements. The storage and loss shear moduli, G' and G'', of all solutions were measured by use of the Birnboim-Schrag multiple lumped resonator (Schrag & Johnson, 1971). A titanium resonator with five working frequencies from 150 to 8000 Hz was used in a titanium resonator housing (Nemoto et al., 1975). A new data acquisition and processing system was used instead of the original system (Schrag & Johnson, 1971). The new system consists of a Data General NOVA 4/S computer with disk storage and a Hewlett-Packard (Model 3325A) waveform generator that sets the variable sampling rate of the computer. The system allows considerable signal averaging, and 40–100 times more averaging was used in this study than was possible with the original system. More details about the system are described elsewhere (Nestler, 1981).

The resonator apparatus was filled slowly by use of a 50-mL syringe equipped with a 15-gauge needle. The housing was normally dry before the solution was filled in, but sometimes the housing was wet with solvent, and the solution was then drained and refilled before the measurements. Concentrations were measured after each run by UV absorption. The apparatus was cleaned with a trypsin solution after measurements, washed several times with buffer and water, soaked in either methanol or ethanol, and dried with nitrogen gas.

After the first solution of each preparation had been measured, subsequent measurements were performed on solutions diluted sequentially with stock solvent. Dialysis against stock solvent was repeated between some measurements to ensure that the solvent viscosity was always the same for the solution

Table I: Solvent Properties and Protein Concentration Ranges Studied

	aqueous solvent (buffer A)	solvent with glycerol (buffer G)
density at 7.0 °C (g/cm³)	1.092	1.242
density at 1.0 °C (g/cm³)		1.244
viscosity at 7.0 °C (cP)	1.683	33.3
viscosity at 1.0 °C (cP)		48.7
native concn range (mg/mL)	1.52–3.48	2.78–10.50
renatured concn range (mg/mL)	0.67–4.38	0.85–3.27

as for the solvent used in instrument calibration.

Measurements were made at 7.0 °C for buffer A solutions and at 1.0 and 7.0 °C for solutions in buffer G. Solution and solvent runs were always made on the same day to minimize small drifts in the calibration of the instrument. The loss and storage moduli are obtained from the frequency shift and the change in bandwidth of the resonances between solvent and solution runs (Schrag & Johnson, 1971). It is convenient to use the reduced storage and loss shear moduli defined respectively as

$$G'_R = [M/(cRT)]G' \quad (1)$$

$$G''_R = [M/(cRT)](G'' - \omega\eta_s) \quad (2)$$

where M is the molecular weight, R the gas constant, T the absolute temperature, c the protein concentration in grams per milliliter, ω the radian frequency of oscillation (2π times frequency in hertz), and η_s the solvent viscosity. Table I summarizes the properties of the solvents used and the concentration ranges studied.

Circular Dichroism. Circular dichroic (CD) spectra were measured at ambient temperatures with a spectropolarimeter (Jasco Model J20) to test the effect of glycerol on the degree of helicity. CD spectra from 210 to 280 nm were taken with a rod concentration of 21.8 μg/mL in 0.5 M K_2HPO_4 adjusted to pH 7.3 with HCl. The solutions also contained varying amounts of glycerol from 0 to 70% by volume. The minimum at 222 nm was taken as a measure of the α helicity, and the mean residue molecular ellipticity was calculated (Nakayama et al., 1980).

Analytical Ultracentrifugation. Sedimentation velocity runs were performed at ambient temperatures on a Beckman Instruments Model E analytical centrifuge, equipped with a UV photoelectric scanner. A 2.1 mg/mL native rod solution and a 1.0 mg/mL renatured rod solution in buffer A were followed at 278 nm at 40 000 and at 44 000 rpm, respectively. The measured sedimentation coefficients were reduced to water at 20 °C by correcting for *solution* viscosity and solvent density. The partial specific volume was taken to be 0.710 cm³/g (Harrington & Burke, 1972). Use of the solution viscosity in this correction provides an approximate estimate of the sedimentation coefficient at infinite dilution.

Results

Characterization of Rod Preparations. The average yield of crude rod was about 500 mg from 400 g of muscle. NaDodSO$_4$ gel electrophoresis of fractions eluted from the hydroxylapatite column showed that the front of the main peak contained considerable amounts of lower molecular weight material. The back two-thirds of the main peak contained primarily rod and was pooled. The apparent molecular weight of each strand of the rod on this gel system was 125 000–130 000. The pooled fractions showed from 5 to 12% lower molecular weight bands for six preparations as judged from the densitometric scans. Figure 1 shows the elution profile

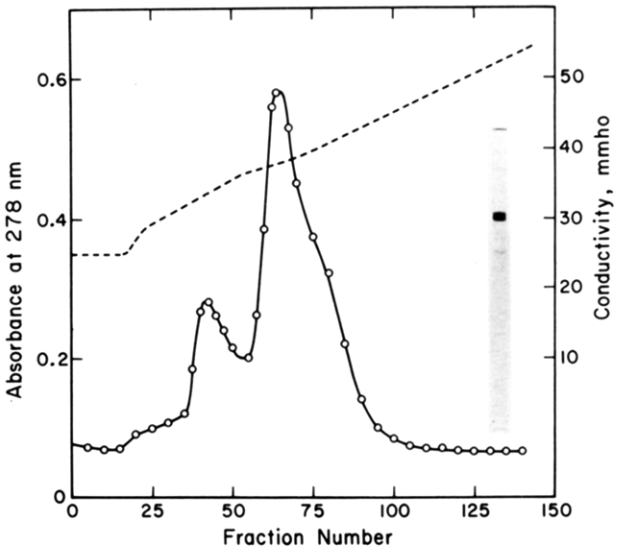

FIGURE 1: Hydroxylapatite chromatography of crude rod solution. (Solid curve) Absorbance at 278 nm (left scale); (dashed curve) solution conductivity (right scale). Only a few of the measured absorbances are shown for clarity. The small peak and the front of the main peak contained some lower molecular weight material. Fractions 65–91 were pooled. NaDodSO$_4$–polyacrylamide gel of the pooled fractions is shown at the right.

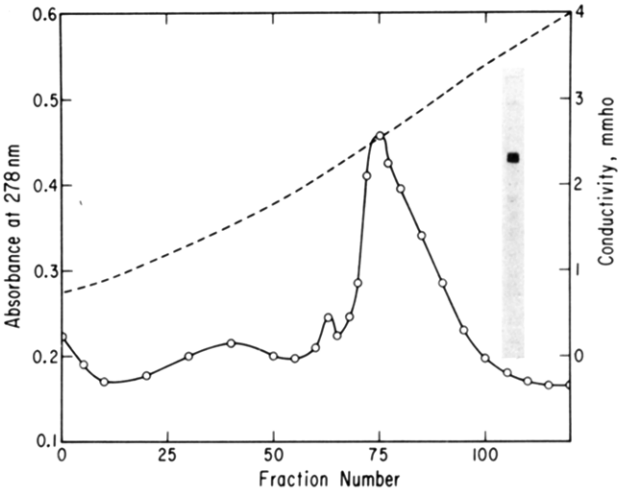

FIGURE 2: DEAE-cellulose chromatography of crude rod solutions in 7 M urea. Curves and points are as in Figure 1. NaDodSO$_4$–polyacrylamide gel of pooled fractions (72–101) is shown to the right.

from the HAP column and a gel of the pooled fractions. The main contaminant was a doublet with an apparent molecular weight of about 90 000. We were not able to remove these contaminants under nondenaturing conditions. Similar contaminants have been observed by others (Margossian et al., 1981).

Chromatography under denaturing conditions allowed a separation of these contaminants, and renatured preparations with more than 96% purity were obtained. A typical elution profile from the DEAE column and a gel of the pooled fractions are shown in Figure 2. The front shoulder of the main peak contained most of the contaminants. Renaturation from solutions with urea has also been observed for the two coiled-coil α-helical proteins tropomyosin (Cummins & Perry, 1973) and paramyosin (Crimmins & Holtzer, 1981).

Both native and renatured rods migrated as a single front in the ultracentrifuge with an estimated infinite dilution sedimentation coefficient of 3.2 S reduced to standard conditions. This value is close to the reported 3.4 S (Oriol et al., 1973). Intrinsic viscosities in the aqueous solvent were measured

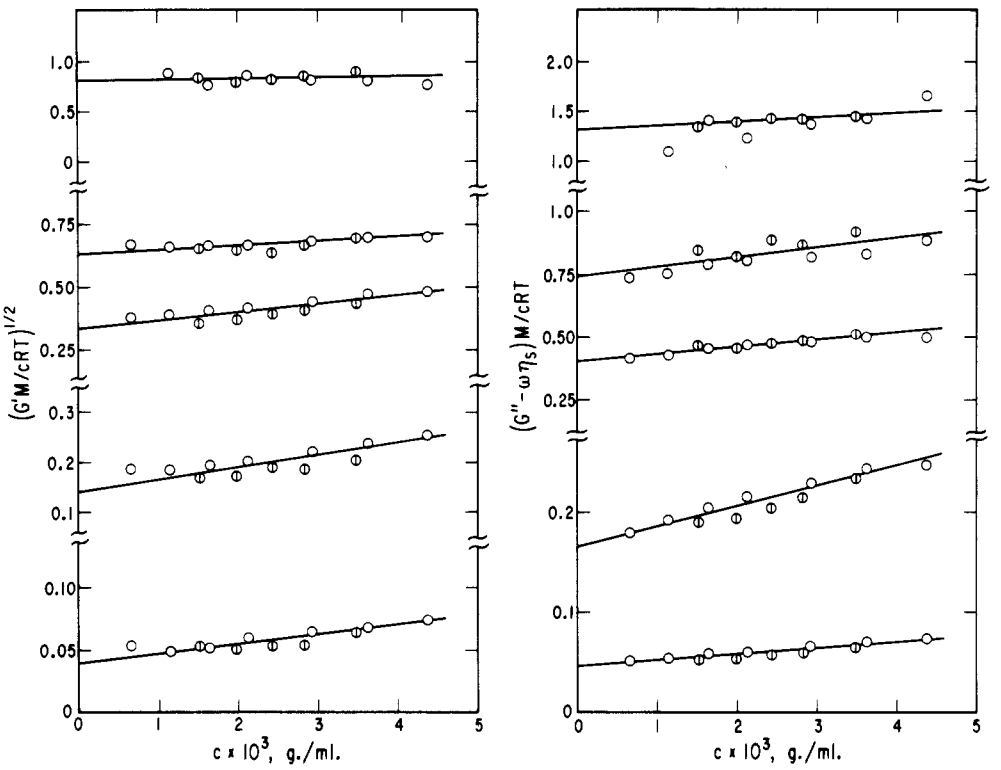

FIGURE 3: Plots of $[G'M/(cRT)]^{1/2}$ and $(G''-\omega\eta_s)M/(cRT)$ against concentration in aqueous solvent at 7.0 °C. The frequencies of measurements are, from bottom to top, 145, 575, 1499, 3757, and 8052 Hz. (Open circles) Renatured preparation; (slotted circles) native preparation.

routinely at 7.0 °C and were in the range 285–302 mL/g for both types of preparations. The average value was 293 mL/g in buffer A and in acceptable agreement with a zero shear-rate intrinsic viscosity of 304 mL/g in buffer G. Inclusion of 1 mM dithiothreitol was found not to change the reduced viscosity of a renatured solution to within 0.5%.

The circular dichroism spectra with varying amounts of glycerol showed that the peak minimum at 222 nm was 88 mdeg for a native rod solution of 21.8 μg/mL in a 1-cm cuvette, independent of the amount of glycerol from 0 to 70%. With the assumption of a mean residue molecular weight of 115 g/mol, this corresponds to a mean residue molecular ellipticity of -4.6×10^4 deg cm^2/dmol, in good agreement with literature values for the rod (Nakayama et al., 1980).

The UV absorption spectra of rod solutions showed a maximum absorption at 277.5 nm both in the aqueous solvent and in the solvent containing glycerol. The extinction coefficient was the same in both solvents to within 0.5%. This was shown by diluting equal volumes of rod solution with either buffer A or buffer G and measuring UV absorbance with solvent references made up the same way. The absorbance at 278 nm was proportional to concentration up to at least 4.5 mg/mL. The ratio of absorbances at 278 to 260 nm was at least 1.95 for both types of column-purified rod solutions, indicating little or no contamination with nucleotides.

Viscoelastic Measurements. The reduced intrinsic storage and loss shear moduli $[G']_R$ and $[G'']_R$ were obtained by extrapolating G''_R and $G'_R{}^{1/2}$ at each frequency to zero concentration (Nemoto et al., 1975). This is illustrated in Figure 3 for the aqueous solutions (buffer A) and in Figure 4 for the solutions containing glycerol (buffer G). The molecular weight was taken as 220 000 (Margossian et al., 1981; Sutoh et al., 1978). The higher apparent molecular weight observed on our gels is characteristic for Laemmli gel systems (Sutoh et al., 1978). The data for native and renatured rod are seen to be in reasonably good agreement in both aqueous and glycerol solvents.

The intrinsic moduli $[G']_R$ and $[G'']_R$ are plotted logarithmically against the conventional reduced frequency, $\omega\eta_s[\eta]M/(RT)$, in Figure 5. Here η_s and $[\eta]$ are the measured capillary solvent viscosity and intrinsic viscosity, respectively. The wide range of reduced frequencies is due to the large variation in solvent viscosities. The data are compared first with theoretical curves (dashed) for a rigid cylinder (Yamakawa, 1975) for which the reduced moduli can be expressed as

$$[G']_R = m_1\omega^2\tau_0^2(1 + \omega^2\tau_0^2)^{-1} \quad (3)$$

$$[G'']_R = \omega\tau_0[m_1(1 + \omega^2\tau_0^2)^{-1} + m_2] \quad (4)$$

$$\tau_0 = m[\eta]\eta_s M/(RT) \quad (5)$$

with $m_1 = 3/5$, $m_2 = 4/(5\gamma) - 3/5$, and $m = 5\gamma/4$. The parameter γ depends slightly on the axial ratio of the cylinder and is 0.91 for the dimensions of the rod (see below). For an infinitely long cylinder, γ is 1.0. The relaxation time (τ_0) corresponds to end over end rotation. A good fit is obtained at low frequencies, but the data at intermediate and high frequencies show marked deviations from the theoretical predictions. Tobacco mosaic virus followed a rigid rod model over a wide range of frequencies (Nemoto et al., 1975).

The data are also compared with the only available model for a hinged rod, the freely jointed three bead model (Hassager, 1974). His calculation shows that the moduli have contributions from two dominant relaxation times. More realistic models for hinged rods are also expected to result in only a few relaxation times due to the few degrees of freedom for a hinged rod. The full curves in Figure 5 are Hassager's intrinsic moduli. It is seen that the agreement is very good for $[G'']_R$ but not for $[G']_R$ at either low or high frequencies. The departure at high frequencies indicates that many relaxation processes are contributing to the viscoelastic properties.

Semiflexible rods give rise to a whole spectrum of bending relaxation times (Barkley & Zimm, 1979), but a rigorous

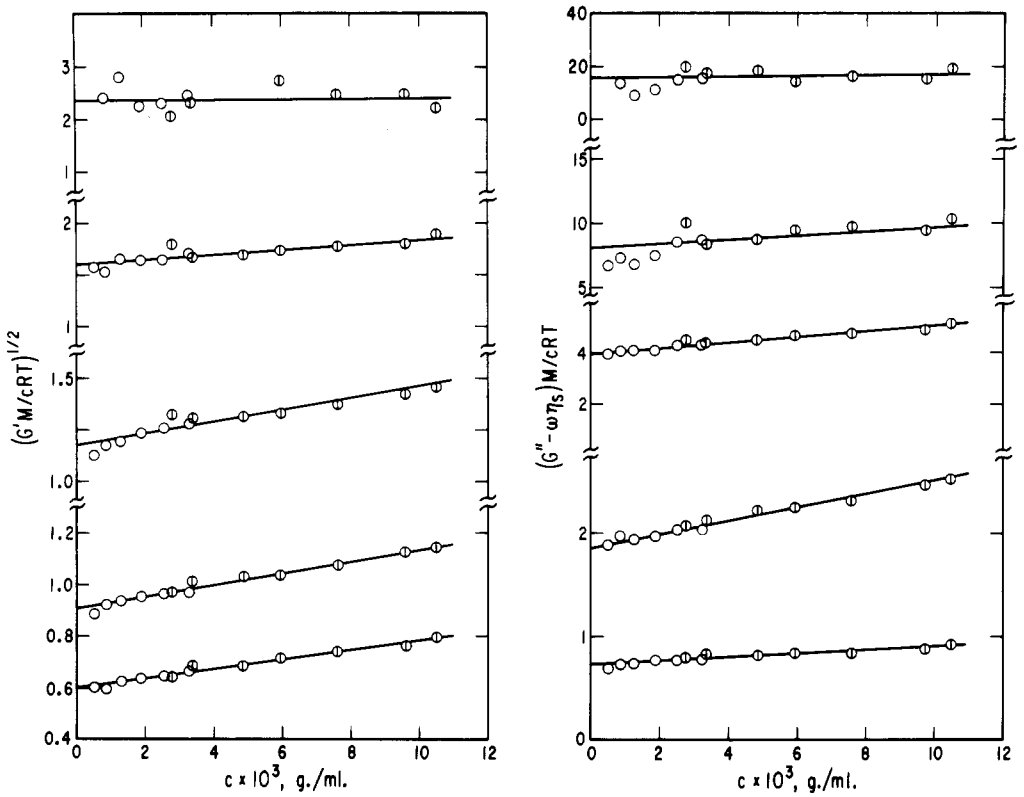

FIGURE 4: Plots of $[G'M/(cRT)]^{1/2}$ and $(G'' - \omega\eta_s)M/(cRT)$ against concentration in solvent containing glycerol at 7.0 °C. The frequencies of measurements are, from bottom to top, 144, 573, 1495, 3752, and 8047 Hz. Symbols are the same as in Figure 3.

theoretical calculation of the viscoelastic properties of semiflexible rods is not available. The empirical hybrid model has been used to describe the behavior of helical molecules such as poly(γ-benzyl-L-glutamate) (Warren et al., 1973) and paramyosin (Rosser et al., 1977) with a frequency dependence as follows:

$$[G']_R = m_1\omega^2\tau_0^2(1 + \omega^2\tau_0^2)^{-1} + Z'(\omega\tau_1) \quad (6)$$

$$[G'']_R = \omega\tau_0[m_1(1 + \omega^2\tau_0^2)^{-1} + m_2] + Z''(\omega\tau_1) \quad (7)$$

where τ_0 was associated with end over end rotation (compare with eq 3 and 4). Z' and Z'' are the reduced moduli specified by the Zimm theory (Zimm, 1956) for flexible random coils (bead-spring model), where τ_1 is the longest Zimm-like relaxation time, attributed to flexural modes of motions of weakly bending rods (Rosser et al., 1977).

The data from Figure 5 were compared with the predictions of the hybrid model with $m_1 = 0.6$. The best fit was obtained with $\tau_0/\tau_1 = 8$ and $m_2 = 0.15$ and is shown in Figure 6. The value of m_2 seems to be typical for moderately long semiflexible helices. The values found for paramyosin and myosin were 0.10 and 0.20, respectively (Rosser et al., 1977, 1978). The value of m_2 is 0.20 for a long rigid cylinder.

The rotational relaxation time τ_0 can be calculated from the fit to the hybrid model. For this model, eq 5 holds (Rosser et al., 1977) with

$$m = (m_1 + m_2 + 2.37\tau_1/\tau_0)^{-1} \quad (8)$$

Reduced to water at 20 °C, τ_0 becomes 25 μs. This value compares favorably with the rotational relaxation time of 23.3 μs at 20 °C determined from electric birefringence measurements at 3 °C (Highsmith et al., 1977). The viscoelastic measurements further show that the characteristic time for the slowest bending motion is 3.1 μs when reduced to water at 20 °C.

Discussion

The virtual agreement of results from the sedimentation and intrinsic viscosity measurements of renatured and native rod preparations suggests that the rod renatured completely within experimental accuracy. The intrinsic viscosity is quite sensitive to small amounts of shorter polypeptides (Harrington & Burke, 1972). The lower molecular weight material observed on $NaDodSO_4$ gels in the native preparations did not give rise to extra sedimenting species in the ultracentrifuge or lower intrinsic viscosities. These contaminants are most likely due to nicking of only one of the polypeptide chains, such that the rod will still appear homogeneous under nondenaturing conditions (Margossian et al., 1981). The findings from the CD measurements and the rather good agreement between the intrinsic viscosities in aqueous solvent and in the solvent containing glycerol were taken as evidence that glycerol does not alter the conformation of the myosin rod. Strong additional support for this interpretation is obtained from the excellent superposition of the two sets of data in Figures 5 and 6.

The degree of flexibility of wormlike chains or semiflexible rods is traditionally given in terms of the persistence length or the bending force constant. The persistence length, q, is a measure of the distance the chain persists along a given direction before changing its course, and the bending force constant, B, is a measure of how much the chain resists bending. It can be shown (Yamakawa, 1971; Bloomfield et al., 1974) that B and q are related through

$$B = qkT \quad (9)$$

where k is Boltzmann's constant.

The viscoelastic measurements show that myosin rod behaves like a semiflexible rod. This conclusion was reached without assigning a length to the rod. Other reasonable choices of the molecular weight would not affect that conclusion either. In order to get quantitative information about the rigidity of

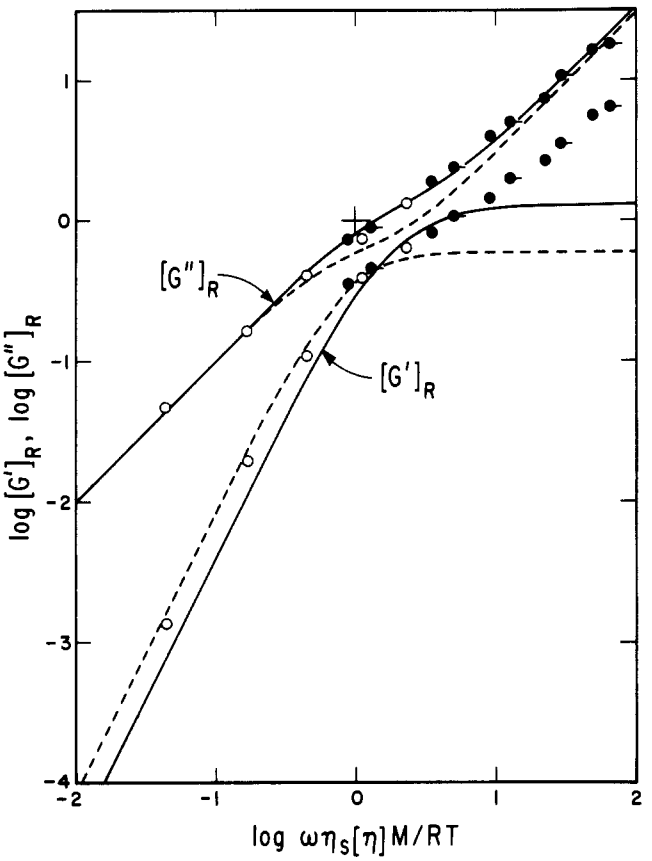

FIGURE 5: Reduced intrinsic moduli, $[G'']_R$ and $[G']_R$, plotted logarithmically against reduced frequency, $\omega\eta_s[\eta]M/(RT)$. (Open circles) Aqueous solvent (buffer A); (closed circles) solvent containing glycerol (buffer G) at 7.0 °C (without pip) and at 1.0 °C (with pip). (Dashed curve) Yamakawa theory for rigid rod; (solid curve) Hassager theory for freely jointed trinodular rod.

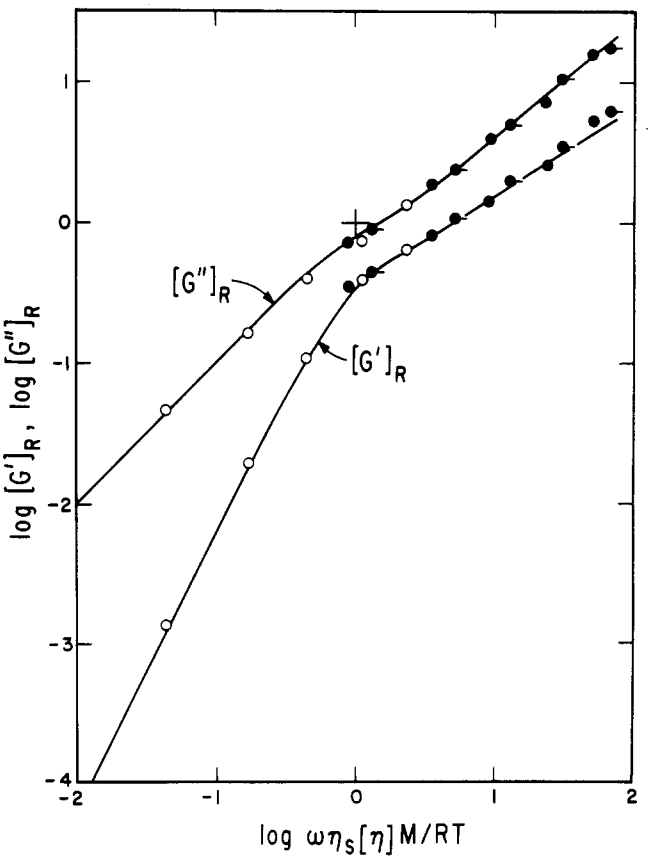

FIGURE 6: Data of Figure 5 compared with hybrid theory (solid curves) with $m_1 = 0.6$, $m_2 = 0.15$, and $\tau_0/\tau_1 = 8$.

the rod, it is necessary to know the contour length, L, of the rod. We have chosen 144 nm (Sutoh et al., 1978) since this value is in agreement with electron microscopy data (Takahashi, 1978) and is consistent with a length calculated by using a molecular weight of 220 000, an amino acid residue weight of 115, and a 0.149-nm translation in the axial direction per residue (Crick, 1953). The diameter of the rod was taken to be 2 nm (Highsmith et al., 1977); the conclusions are not very sensitive to the value chosen except for the estimate of Young's modulus (see later).

An analysis of flexure was made by Ookubo et al. (1976), and they showed that the flexural time, τ_F, associated with the fundamental flexural mode is related to the persistence length of semiflexible rods by

$$\tau_F = (5.53 \times 10^{-3})\frac{\pi\eta_s L^4}{qkT \ln (L/d)} \qquad (10)$$

Identifying our longest flexural relaxation time τ_1 with τ_F, we obtain from the dimensions of the rod a persistence length of 138 nm, which corresponds to a bending force constant of 5.6×10^{-28} Nm^2 at 20 °C. Two other estimates of the persistence length can be obtained from the values of τ_0 and $[\eta]$. The rotational relaxation time for a long semiflexible chain of touching beads has recently been calculated as a function of L, d, and q (Hagerman & Zimm, 1981). From the dimensions of the rod and a τ_0 of 25 μs, the persistence length has been calculated and is listed in Table II. The intrinsic viscosity of a smooth flexible cylinder with hemispherical caps at the ends has been calculated as a function of M, L, d, and q (Yamakawa & Yoshizaki, 1980). A rigid cylinder (q infinite) with the dimensions of the rod and a molecular weight of 220 000 should have an intrinsic viscosity of 348 mL/g. From the measured value of 293 mL/g, another estimate of the persistence length was obtained, and it is also given in Table II. The persistence length of paramyosin has been calculated by use of eq 10 from the measured τ_1 of 2.7 μs at 20 °C (Rosser et al., 1977) by assuming a molecular weight of 210 000 and an estimated length of 137.5 nm.

Table II: Persistence Length of Helical Macromolecules

macromolecule	type of measurement[a]	persistence length (nm)
myosin rod[b]	τ_F	138
myosin rod[b]	$[\eta]$	148
myosin rod[b]	τ_0	115
paramyosin[c]	τ_F	135
DNA[d]	τ_0	50
collagen[e]	$[\eta]$	130

[a] τ_F, $[\eta]$, and τ_0 denote longest flexural time, intrinsic viscosity, and rotational relaxation time, respectively. [b] This study. [c] Results from Rosser et al. (1977). Recalculated as described in the text. [d] Results from Hagerman (1981). [e] Results from Utiyama et al. (1973).

The persistence lengths of double-stranded DNA in high salt solutions and of triple-stranded collagen are also shown for comparison in table II. It is seen that the three estimates of myosin rod persistence length are in quite good agreement in view of the different models and assumptions used in the calculations and the uncertainties in the contour length and extinction coefficient which are used. The rod persistence length of 130 ± 20 nm is very similar to the value found for paramyosin, and it suggests that a persistence length of about 130 nm may be characteristic for double-stranded coiled-coil α-helical proteins. It is remarkable that myosin rod is more

than twice as stiff as DNA and is comparable to collagen.

It should be remembered that we have analyzed our low-temperature viscoelastic data in terms of a semiflexible rod with the same flexibility along its entire length. Hydrodynamic data of myosin have also been interpreted in support of a model with a hinge between rigid subfragments LMM and S-2 (García de la Torre & Bloomfield, 1980; Highsmith et al., 1977). Our viscoelastic data do not support such a model. We cannot rule out the possibility that LMM is rigid and only S-2 is flexible. This possibility was also considered by Highsmith et al. (1977). It seems very unlikely, however, since that would make LMM unrealistically rigid when compared with paramyosin, and the persistence length of S-2 would become only about 7 nm as estimated from eq 10 with $\tau_F = 3.1$ μs and a length of S-2 equal to 65 nm (Sutoh et al., 1978). It seems, therefore, unlikely that the rod is flexible only in the S-2 subfragment, and indeed viscoelastic measurements show that LMM behaves as a semiflexible rod with a flexibility very similar to that of the entire rod (S. Hvidt, unpublished experiments).

The possibility that the rod could be hinged with semiflexible subfragments deserves consideration. It seems likely that such a model could predict curves of the reduced moduli that would fit the data in Figures 5 and 6 quite well, but such a model would predict much too small an intrinsic viscosity. Wilemski (1977) has calculated the intrinsic viscosity of a once-broken rod and has shown that the ratio of intrinsic viscosities for a freely jointed once-broken rod to a rigid rod is approximately $1 - 6[\sigma(1 - \sigma)]^2$, where σ denotes the position of the hinge relative to the entire length of the rod. With a hinge between S-2 and LMM (79 nm) and a total contour length of 144 nm, σ becomes 0.55, which leads to a predicted intrinsic viscosity of 219 mL/g. A semiflexible hinged rod is expected to have an even lower intrinsic viscosity. The measured value seems to rule out the applicability of this model. We believe that the simplest model that can describe all the low-temperature properties is a semiflexible rod with the same flexibility along the entire rod, although we cannot rule out strictly the possibility of a semiflexible rod with a hinge that allows only very restricted motions.

The persistence length for the rod of about 130 nm shows that the coiled-coil α helices are very rigid structures, but considerable movements of the ends of the rod are allowed due to its long length. We can obtain an estimate of the root mean square excursion, $\langle y^2 \rangle^{1/2}$, due to thermal fluctuations of one end of the rod when the other end is held fixed as illustrated in Figure 7. The elastic energy of a bent rod is set equal to $^1/_2 kT$ and solved for y following ideas by Ookubo et al. (1976):

$$\langle y^2 \rangle^{1/2} = \left(\frac{L^3}{3q} \right)^{1/2} \tag{11}$$

The root mean square excursion for the free end of the rod is 87.5 nm for $L = 144$ nm and $q = 130$ nm with a similar excursion in a perpendicular direction. Light meromyosin is known to aggregate at low ionic strength. The dimer is stabilized by a least $10kT$ with respect to the monomer even in a solvent containing 0.5 M KCl, 0.2 M phosphate (pH 7.3), and 10 mM EDTA (Harrington & Burke, 1972). LMM is therefore immobilized in muscles under physiological conditions due to the attractive forces between LMM and neighboring myosin molecules in the thick filament shaft. Subfragment 2 shows much less tendency to aggregate, and small changes in pH can release S-2 from its resting state near the thick filament (Sutoh et al., 1978). Once it is released from the thick filament, the root mean square excursion can be

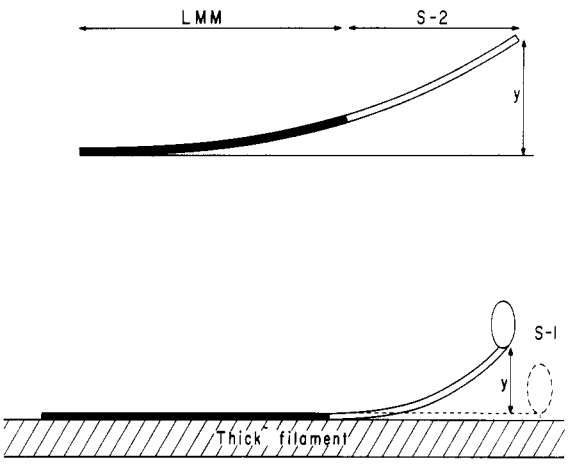

FIGURE 7: Flexibility of myosin rod. Top figure: rod in solution; y denotes excursion of one end relative to the tangent of the other end during flexible motion. Bottom figure: myosin in thick filament; LMM is immobilized and is held close to the shaft of the filament. The resting position of S-2 and S-1 is illustrated by dashed figure. Excursion perpendicular to the shaft of the filament after HMM is released from the shaft is illustrated by solid figure. Only one myosin head is shown.

estimated by use of eq 11, taking $L = 65$ nm (Sutoh et al., 1978) and $q = 130$ nm. We obtain $\langle y^2 \rangle^{1/2}$ for the free end of S-2 to be 26.5 nm. The two myosin heads which are attached to the end of S-2 are therefore allowed considerable excursions perpendicular to the shaft of the thick filament. It seems most unlikely that the rod will be less flexible at physiological temperatures so excursions at least as big are expected at 37 °C. The hinge between LMM and S-2 was postulated by Huxley (1969) in order to allow HMM to span the gap between the thin and thick filaments and to accommodate for the increased filament–filament distance of about 4 nm at short sarcomere lengths. Our results show that is is unnecessary to require such a hinge since S-2 is flexible enough to span the gap at all sarcomere lengths just due to thermal motions.

Electron microscopy of native filaments (Trinick & Elliott, 1979) showed that the distance between the surface of the thick filament and the part of the myosin heads most distant from the filament varied between 20 and 50 nm. They further showed that the myosin heads appeared to be about 19 nm long and 7 nm wide. We predicted a distribution of excursions, y, with a thermal average of 26 nm for the S-1/S-2 junction, from the flexibility of the rod. The average excursion of the most distant part of the myosin heads must therefore be between 26 and 45 nm, where the upper limit corresponds to one of the freely rotating heads pointing directly away from the filament, as illustrated in Figure 7. The lower limit corresponds to both heads pointing in toward the filament such that the most distant part of the heads is near the S-1/S-2 junction. The predicted range is in good agreement with the findings from electron microscopy.

A rigorous calculation of the flexural times for the bending motions of HMM when LMM is immobilized is complicated by the presence of the myosin heads and by the fact that the end of S-2, next to LMM, is held fixed as illustrated in Figure 7. The flexural time associated with the slowest flexural mode of free S-2 in solution can be calculated by use of eq 10 to be 0.16 μs at 20 °C. The myosin heads will undoubtedly increase the time for the slowest bending mode of S-2 in HMM. The slowest bending time for myosin in solution was found to be 6.3 μs (Rosser et al., 1978) compared with the bending time of 3.1 μs for the rod in solution. The longest flexural time of a rod with one end fixed can be calculated (S. Hvidt, un-

published results) following the ideas of Ookubo et al. (1976) which led to eq 10 for a rod with free ends. The same result is obtained for the rod with one end fixed except that $(5.53 \times 10^{-3})/[\ln (L/d)]$ has to be replaced by $3/[8 \ln (2L/d)]$, such that the longest bending time constant for S-2 with immobilized LMM becomes 9 μs at 20 °C. The longest flexural time of HMM in the thick filament can then be estimated to be about 18 μs, if it is assumed that the heads double the flexural time for S-2 as they did for the rod. The estimated bending time for HMM is very short compared with the cross-bridge cycle time, which is estimated to be in the millisecond range (Huxley & Simmons, 1971) or even near 500 ms (Borejdo et al., 1979). It is perhaps fortuitous that our flexural times are very similar to the correlation times determined from electron paramagnetic resonance studies on labeled S-1 (Thomas et al., 1975, 1980). They observed times of about 10 μs for myosin in filaments and that the motions were about 10 times faster for myosin in solution. They attributed these motions to rotation of the heads. These times are, however, also in the range we would expect for motions of the heads due to the flexibility of the helical parts of myosin. Additional experiments seem necessary in order to test the two interpretations.

The S-2 fragment is the mechanical link between the thin and thick filaments when the myosin heads are attached to the actin. The fragment transmits the tension between the rotating myosin heads and the thick filament in the Huxley–Simmons model. Early tension responses to sudden length changes showed an elastic element within either the myosin heads or S-2. The stiffness of this element was calculated to be 2.5×10^{-4} N/m, and the element should be stretched up to 12 nm during the power stroke (Huxley & Simmons, 1971). More recent estimates show a stretching of 4–6 nm (Ford et al., 1977). The viscoelastic measurements allow an estimate of the stiffness of S-2 in stretching. Young's modulus, E, is defined as the stress divided by strain in simple extension, and it is related to the bending force constant and the diameter of an elastic rod through

$$E = \frac{64B}{\pi d^4} \tag{12}$$

An estimate of E is obtained if d is taken as 2 nm. We find $E = 6.7 \times 10^8$ N/m^2 with $q = 130$ nm by use of eq 9 and 12. If the rod is modeled as two helices each with a diameter of 1 nm, E becomes 1.3×10^9 N/m^2. These values are very high and characteristic for a polymer in the glassy zone (Ferry, 1980). The stiffness of S-2, 3.2×10^{-2} N/m, is obtained from E, the cross-sectional area, and an S-2 length of 65 nm. This value is about 130 times higher than the stiffness calculated from the Huxley–Simmons model. The elastic element must therefore be a part of the myosin heads unless a conformational change, like a helix–coil melting, takes place in S-2 as proposed by Harrington (1979b). Our low-temperature viscoelastic measurements do not allow a distinction between these two possibilities, but it seems unlikely that such a significant stretching could take place within the size of the heads which are about 14 nm long. Saturation transfer electron paramagnetic resonance measurements (Thomas et al., 1975) showed no flexibility within the heads. There is physicochemical evidence, on the other hand, that a part of S-2 is less stable near physiological temperatures than the rest of the rod (Burke et al., 1973; Tsong et al., 1979).

Acknowledgments

We greatly appreciate valuable discussions with Paul A. Janmey, Lawrence D. Yates, Dr. Richard L. Moss, and Professor J. L. Schrag. We are further indebted to Professor Hyuk Yu and Professor M. Thomas Record, Jr., for generous use of some of their equipment. The assistance of Joy Lang and Candace Cook with some of the calculations is acknowledged.

References

Barkley, M. D., & Zimm, B. H. (1979) *J. Chem. Phys. 70*, 2991–3017.

Bloomfield, V. A., Crothers, D. A., & Tinoco, I., Jr. (1974) *Physical Chemistry of Nucleic Acids*, Chapter 5, Harper and Row, New York.

Borejdo, J., Putnam, S., & Morales, M. F. (1979) *Proc. Natl. Acad. Sci. U.S.A. 76*, 6346–6350.

Burke, M., Himmelfarb, S., & Harrington, W. F. (1973) *Biochemistry 12*, 701–710.

Crick, F. H. C. (1953) *Acta Crystallogr. 6*, 689–697.

Crimmins, D. L., & Holtzer, A. (1981) *Biopolymers 20*, 925–980.

Cummins, P., & Perry, S. V. (1973) *Biochem. J. 133*, 765–777.

Ferry, J. D. (1978) *Pure Appl. Chem. 50*, 299–308.

Ferry, J. D. (1980) *Viscoelastic Properties of Polymers*, 3rd ed., Wiley, New York.

Ford, L. E., Huxley, A. F., & Simmons, R. M. (1977) *J. Physiol. (London) 269*, 441–515.

García de la Torre, J., & Bloomfield, V. A. (1980) *Biochemistry 19*, 5118–5123.

Hagerman, P. J. (1981) *Biopolymers 20*, 1503–1535.

Hagerman, P. J., & Zimm, B. H. (1981) *Biopolymers 20*, 1481–1502.

Harrington, W. F. (1979a) *Proteins (3rd Ed.) 4*, 245–409.

Harrington, W. F. (1979b) *Proc. Natl. Acad. Sci. U.S.A. 76*, 5066–5070.

Harrington, W. F., & Burke, M. (1972) *Biochemistry 11*, 1448–1455.

Harrington, W. F., & Himmelfarb, S. (1972) *Biochemistry 11*, 2945–2952.

Harvey, S. C., & Cheung, H. C. (1977) *Biochemistry 16*, 5181–5187.

Harvey, S. C., & Cheung, H. C. (1982) in *Cell and Muscle Motility* (Dowben, R. M., & Shay, F. W., Eds.) Vol. 2, pp 279–302, Plenum Press, New York.

Hassager, O. (1974) *J. Chem. Phys. 60*, 4001–4008.

Highsmith, S., Kretzschmar, K. M., O'Konski, C. T., & Morales, M. F. (1977) *Proc. Natl. Acad. Sci. U.S.A. 74*, 4986–4990.

Houk, T. W., Jr., & Ue, K. (1974) *Anal. Biochem. 62*, 66–74.

Huxley, A. F., & Simmons, R. M. (1971) *Nature (London) 233*, 533–538.

Huxley, H. E. (1969) *Science (Washington, D.C.) 164*, 1356–1366.

Kobayashi, S., & Totsuka, T. (1975) *Biochim. Biophys. Acta 376*, 375–385.

Laemmli, U. K. (1970) *Nature (London) 227*, 680–685.

Lovell, S. J., & Harrington, W. F. (1981) *J. Mol. Biol. 149*, 659–674.

Lowey, S. (1971) in *Subunits in Biological Systems* (Timasheff, S. N., & Fasman, G. D., Eds.) pp 201–259, Marcel Dekker, New York.

Lowey, S., Slayter, H. S., Weeds, A. G., & Baker, H. (1969) *J. Mol. Biol. 42*, 1–29.

Margossian, S. S., Stafford, W. F., III, & Lowey, S. (1981) *Biochemistry 20*, 2151–2155.

Mendelson, R. A., Morales, M. F., & Botts, J. (1973) *Biochemistry 12*, 2250–2255.

Nakayama, T., Suzuki, Y., Niwa, E., & Hamada, I. (1980) *Agric. Biol. Chem. 44*, 2363–2369.
Nemoto, N., Schrag, J. L., Ferry, J. D., & Fulton, R. W. (1975) *Biopolymers 14*, 409–417.
Nestler, F. H. M. (1981) Ph.D. Thesis, University of Wisconsin—Madison, Madison, WI.
Ookubo, N., Komatsubara, M., Nakajima, H., & Wada, Y. (1976) *Biopolymers 15*, 929–947.
Oriol, C., Landon, M. F., & van Thoai, N. (1973) *Biochem. Biophys. Res. Commun. 51*, 1023–1026.
Rosser, R. W., Schrag, J. L., Ferry, J. D., & Greaser, M. (1977) *Macromolecules 10*, 978–980.
Rosser, R. W., Nestler, F. H. M., Schrag, J. L., Ferry, J. D., & Greaser, M. (1978) *Macromolecules 11*, 1239–1242.
Schrag, J. L., & Johnson, R. M. (1971) *Rev. Sci. Instrum. 42*, 224–232.
Sutoh, K., Sutoh, K., Karr, T., & Harrington, W. F. (1978) *J. Mol. Biol. 126*, 1–22.
Swenson, C. A., & Ritchie, P. A. (1980) *Biochemistry 19*, 5371–5375.
Takahashi, K. (1978) *J. Biochem. (Tokyo) 83*, 905–908.
Thomas, D. D., Siedel, J. C., Hyde, J. S., & Gergely, J. (1975) *Proc. Natl. Acad. Sci. U.S.A. 72*, 1729–1733.
Thomas, D. D., Ishiwata, S., Seidel, J. C., & Gergely, J. (1980) *Biophys. J. 32*, 873–889.
Trinick, J., & Elliott, A. (1979) *J. Mol. Biol. 131*, 133–136.
Tsong, T. Y., Karr, T., & Harrington, W. F. (1979) *Proc. Natl. Acad. Sci. U.S.A. 76*, 1109–1113.
Utiyama, H., Sakato, K., Ikehara, K., Setsuiye, T., & Kurata, M. (1973) *Biopolymers 12*, 53–64.
Warren, T. C., Schrag, J. L., & Ferry, J. D. (1973) *Biopolymers 12*, 1905–1915.
Weeds, A. G., & Pope, B. (1977) *J. Mol. Biol. 111*, 129–157.
Wilemski, G. (1977) *Macromolecules 10*, 28–34.
Yamakawa, H. (1971) *Modern Theory of Polymer Solutions*, pp 52–56, Harper and Row, New York.
Yamakawa, H. (1975) *Macromolecules 8*, 339–342.
Yamakawa, H., & Yoshizaki, T. (1980) *Macromolecules 13*, 633–643.
Zimm, B. H. (1956) *J. Chem. Phys. 24*, 269–278.

Interactions between the Mitochondrial Adenosinetriphosphatase and Periodate-Oxidized Adenosine 5′-Triphosphate, an Affinity Label for Adenosine 5′-Triphosphate Binding Sites†

Peter N. Lowe* and R. Brian Beechey

ABSTRACT: Periodate-oxidized ATP (o-ATP) was prepared as an affinity label of nucleotide binding sites on the chloroform-released ox heart mitochondrial ATPase. In the presence of $MgSO_4$, o-ATP is a substrate for the ATPase. It can act as a reversible, competitive inhibitor of ATPase activity and can also induce an irreversible inhibition of ATPase activity. In parallel with the irreversible inhibition, covalent incorporation of [^{3}H]o-ATP occurs. ATPase has about 1.05 mol of o-ATP bound per mol of ATPase when the enzyme is 50% inhibited. Most of the covalently bound o-ATP is associated with the α and β subunits and is equally distributed between them. The incorporation of o-ATP into the ATPase is reduced, and the irreversible inhibition induced by o-ATP can be prevented totally by MgADP, MgATP, EDTA/ATP, or EDTA. The location, number, and the functional significance of the o-ATP binding sites are discussed. o-ATP can decompose to form an adenine-containing compound and the tripolyphosphate anion in a β-elimination reaction mechanism. The structures of the adenine-containing compound and its borohydride reduction product were determined. The adenine-containing elimination product inhibited the mitochondrial ATPase activity at a rate greater than that observed with o-ATP. The nature and mechanism of the inhibition of ATPase activity exerted by o-ATP and the elimination product were examined. The significance of the β-elimination reaction to the use of periodate-oxidized nucleotides as affinity labels of nucleotide binding sites on other proteins is discussed.

A common feature of preparations of mitochondrial ATPase (Senior, 1979) is that they possess multiple nucleotide binding sites (Harris, 1978). One or more of these may be catalytic; others may serve regulatory or structural roles (Slater et al., 1979). Although a number of nucleotide analogues have been used to affinity label nucleotide binding sites on the soluble heart mitochondrial ATPase, few, if any, are confirmed catalytically active site directed inhibitors (Russell et al., 1976; Drutsa et al., 1979; Slater et al., 1979; Di Pietro et al., 1979; Lunardi & Vignais, 1979; Kozlov & Milgrom, 1980). This is because either they are not substrates or the labeling has been carried out under conditions where the hydrolysis of ATP does not occur, e.g., in the absence of Mg^{2+}.

The application of periodate-oxidized ATP (o-ATP)[1] to the labeling of sites on the ox heart mitochondrial ATPase has been reported briefly (Lowe et al., 1979b). In this paper, we extend this work. We present results suggesting that o-ATP may label specifically a catalytic site (1 mol/mol of ATPase)

† From the Department of Biochemistry, Chelsea College, London, SW3 6LX, United Kingdom, and Sittingbourne Research Centre, Sittingbourne, Kent, ME9 8AG, United Kingdom. *Received February 3, 1982.* P.N.L. received support from the Science Research Council (CASE).

* Address correspondence to this author at the Department of Biochemistry, University of Cambridge, Cambridge, CB2 1QW, United Kingdom.

[1] Abbreviations: o-ATP, o-ADP, o-AMP, o-adenosine, and o-CTP, periodate-oxidized ATP, ADP, AMP, adenosine, and CTP, respectively; $NaDodSO_4$, sodium dodecyl sulfate; EDTA, ethylenediaminetetraacetic acid; Tris, tris(hydroxymethyl)aminomethane; Hepes, *N*-(2-hydroxyethyl)piperazine-*N*′-2-ethanesulfonic acid.

0006-2960/82/0421-4073$01.25/0